SUPPLEMENTAL MATERIAL

Shi et al., http://www.jem.org/cgi/content/full/jem.20110278/DC1

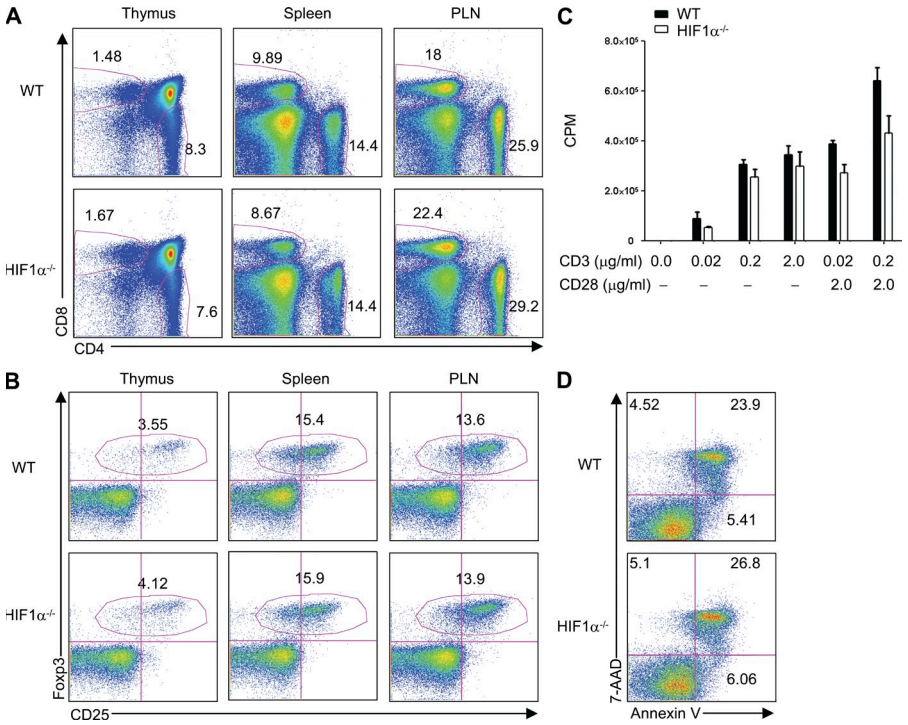

Figure S1. Normal development, proliferation, and survival of HIF1α–deficient T cells. (A) Distribution of CD4 and CD8 cells in the thymus, spleen, and peripheral LNs (PLNs) of WT and HIF1α$^{-/-}$ mice. (B) Proportions of Foxp3^{+} thymic-derived T_{reg} cells among total CD4 T cells in the thymus, spleen, and PLN of WT and HIF1α$^{-/-}$ mice. (C) Proliferation of WT and HIF1α$^{-/-}$ naive cells upon stimulation with anti-CD3 with or without anti-CD28 for 3 d, pulsed for the final 12 h with [^{3}H]-thymidine for thymidine incorporation assays. Data represent the mean ± SEM. (D) Survival of WT and HIF1α$^{-/-}$ naive T cells upon stimulation with anti-CD3/CD28 for 48 h, as measured by Annexin V and 7-AAD staining.

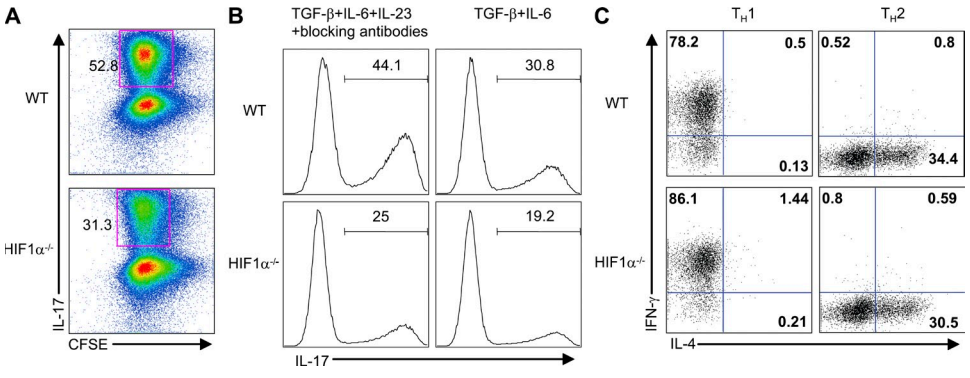

Figure S2. Effects of HIF1α deficiency on effector T cell differentiation. (A) Naive T cells from WT or HIF1α$^{-/-}$ mice were labeled with CFSE and differentiated under T_H17 conditions, followed by intracellular staining of IL-17. (B) Naive T cells from WT or HIF1α$^{-/-}$ mice were differentiated in the presence of TGF-β + IL-6 + IL-23 (plus anti–IL-2, –IL-4, and IFN-γ) or TGF-β + IL-6, followed by intracellular staining of IL-17. (C) Naive T cells from WT or HIF1α$^{-/-}$ mice were differentiated under T_H1 or T_H2 conditions, followed by intracellular staining of IL-4 and IFN-γ.

Database Category (DAVID)	*p* value
BP GO:0006006~glucose metabolic process	8.06E-15
BP GO:0019318~hexose metabolic process	1.51E-14
BP GO:0005996~monosaccharide metabolic process	2.90E-13
PIR glycolysis	3.52E-12
BP GO:0006096~glycolysis	1.74E-11
KEGG mmu00010:Glycolysis/Gluconeogenesis	9.06E-11
BP GO:0006007~glucose catabolic process	2.30E-10
BP GO:0019320~hexose catabolic process	2.30E-10
BP GO:0046365~monosaccharide catabolic process	3.06E-10
BP GO:0044275~cellular carbohydrate catabolic process	1.46E-09

Figure S3. Enrichment of glycolytic and metabolic pathways in HIF1α target genes. Naive T cells from WT and HIF1$\alpha^{-/-}$ mice were differentiated under T_H17 conditions for 2.5 d and subjected to gene profiling analysis. Genes with twofold or greater differences and with false discovery rate <0.05 were analyzed for the enrichment of gene ontology (GO) and canonical pathways using the DAVID bioinformatics databases.

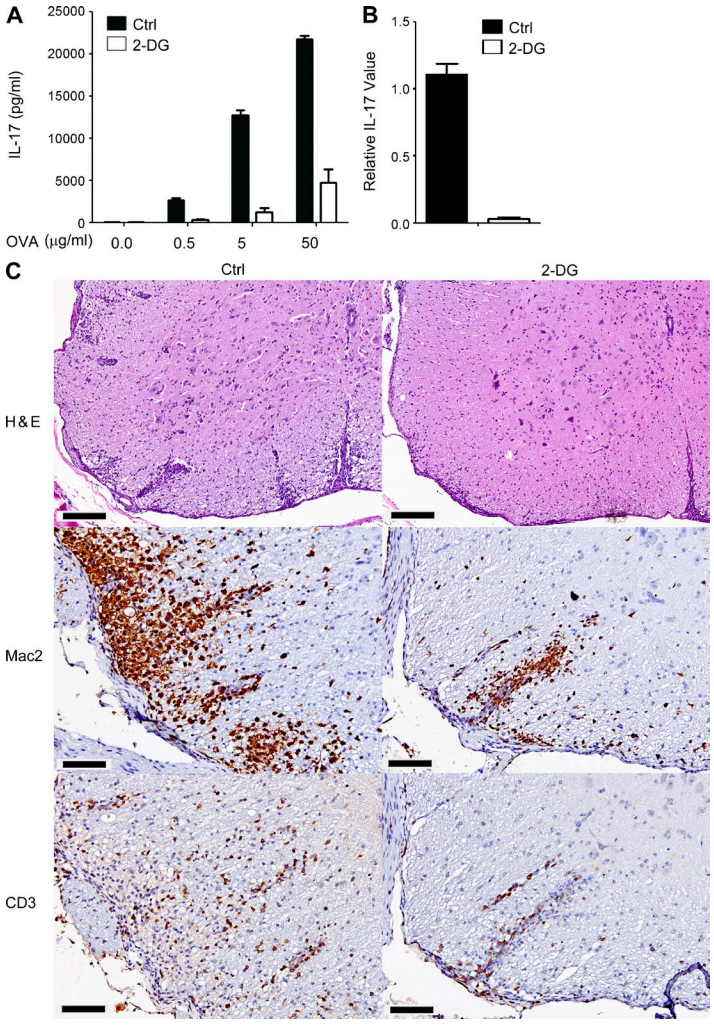

Figure S4. Treatment of 2-DG diminishes T_H17 differentiation and EAE pathogenesis. (A and B) Naive OT-II T cells (Thy1.1$^+$) cells were transferred into C57BL/6 mice and immunized with OVA, with daily treatment of 2-DG or vehicle controls. After 6 d, DLN cells were restimulated with OVA for 2–3 d for the measurements of antigen-specific IL-17 secretion (A) and mRNA expression (B). Data represent the mean ± SEM. (C) C57BL/6 mice were immunized with MOG/CFA and, 9 d later, DLN cells were expanded with MOG and IL-23 in the presence or absence of 2-DG for 5 d, followed by transfer into C57BL/6 mice for the induction of T_H17-polarized transfer EAE. After 12 d, cervical spinal cord sections were analyzed by H&E (bars, 100 μm) and anti-Mac2 and anti-CD3 immunohistochemistry (bars, 200 μm).

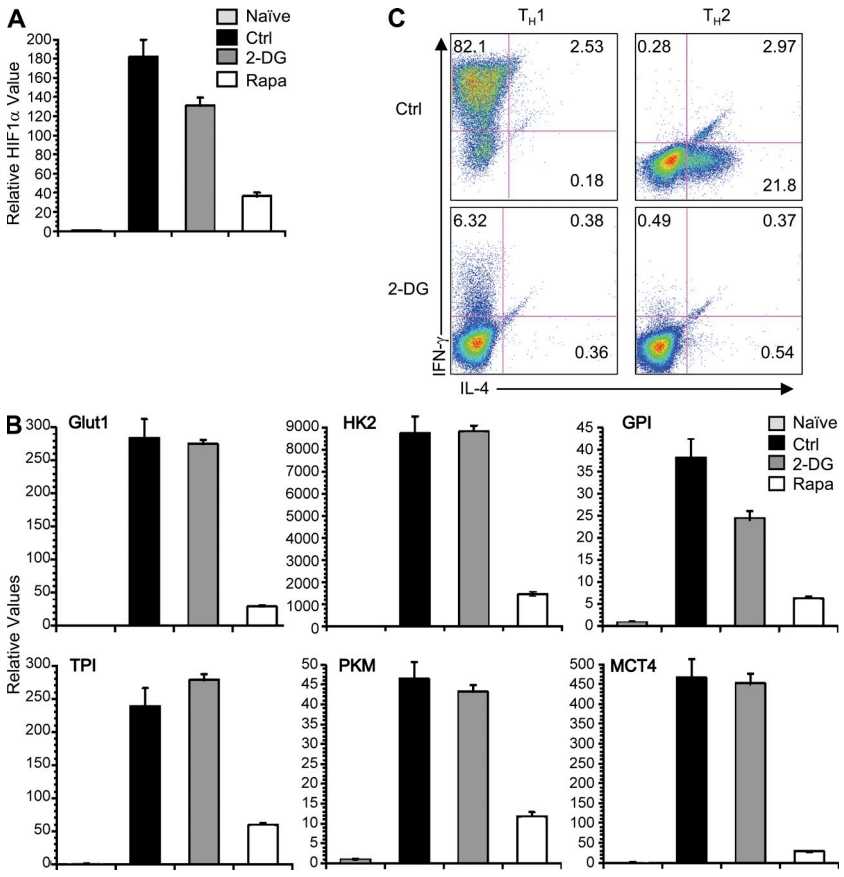

Figure S5. Effects of 2-DG treatment on gene expression and effector T cell differentiation. (A and B) Naive T cells were treated with vehicle (Ctrl), 1 mM 2-DG, or 50 nM rapamycin (Rapa) and differentiated under T_H17 conditions for 2.5 d. Expression of HIF1α (A) and selected glycolytic molecules (B) were examined by real-time PCR analyses (levels in naive cells were set to 1). Data represent the mean ± SD. (C) Naive T cells were treated with vehicle (Ctrl) or 1 mM 2-DG and were differentiated under T_H1 or T_H2 conditions, followed by intracellular staining of IL-4 and IFN-γ.

An Excel file is also provided that contains Table S1.